Electrochemical metal recycling

Oladeji, Abiola; Courtney, James; Fernandez-Villamarin, Marcos; Rees, Neil

[Link to publication on Research at Birmingham portal](#)

Article

Electrochemical Metal Recycling: Recovery of Palladium from Solution and In Situ Fabrication of Palladium-Carbon Catalysts via Impact Electrochemistry

Abiola V. Oladeji, James M. Courtney, Marcos Fernandez-Villamarin, and Neil V. Rees*

Cite This: https://doi.org/10.1021/jacs.2c08239

Read Online

ACCESS | 📊 Metrics & More | 📖 Article Recommendations | 🔵 Supporting Information

ABSTRACT: Recycling of critical materials, regeneration of waste, and responsible catalyst manufacture have been repeatedly documented as essential for a sustainable future with respect to the environment and energy production. Electrochemical methods have become increasingly recognized as capable of achieving these goals, and "impact" electrochemistry, with the advantages associated with dynamic nanoelectrodes, has recently emerged as a prime candidate for the recovery of metals from solution. In this report, the nanoimpact technique is used to generate carbon-supported palladium catalysts from low-concentration palladium(II) chloride solutions (i.e., a waste stream mimic) as a proof of concept. Subsequently, the catalytic properties of this material in both synthesis (Suzuki coupling reaction) and electrocatalysis (hydrogen evolution) are demonstrated. Transient reductive impact signals are shown and analyzed at potentials negative of +0.4 V (vs SCE) corresponding to the onset of palladium deposition in traditional voltammetry. Direct evidence of Pd modification was obtained through characterization by environmental scanning electron microscopy/energy-dispersive X-ray spectroscopy, inductively coupled plasma mass spectrometry, X-ray photoelectron spectroscopy, transmission electron microscopy, and thermogravimetric analysis of impacted particles. This showed the formation of deposits of Pd0 partially covering the 50 nm carbon black particles with approximately 14% Pd (wt %) under the conditions used. This material was then used to demonstrate the conversion of iodobenzene into its biphenyl product (confirmed through nuclear magnetic resonance) and the successful production of hydrogen as an electrocatalyst under acidic conditions (under cyclic voltammetry).
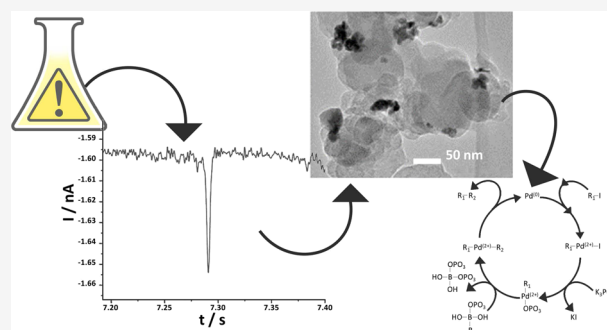
1. INTRODUCTION

Platinum group metals (PGMs) are significant critical metals because of their wide range of applications, most notably as catalysts.[1-3] Palladium is a common catalyst, utilized in many applications and processes such as environmentally important automotive catalytic converters, future energy use in hydrogen storage and production, and large-scale chemical synthesis.[4-15] The Suzuki coupling reaction for example is an industrially important reaction frequently used in pharmaceutical drug synthesis, the formulation of agrochemicals, and polymer production.[16-28]

To improve both performance and economic use, PGM catalysts are often used as supported nanoparticles (NPs), where the support particles disperse the catalytic material to a greater extent, increasing exposure of the catalytic surface area. Carbon materials such as carbon black (CB), graphite, and graphene have been extensively studied as supports,[6,29-37] as they are inexpensive and possess useful properties such as a high electrical conductivity and large surface areas while being mechanically and chemically stable.[38-45]

Pd-modified carbon nanostructured catalysts are extensively used in a range of applications: from electrochemical sensors and organic synthesis to the oxidation of formic acid and reduction of oxygen in fuel cells.[46-59] However, the use of Pd can lead to environmental pollution via release of contaminated waste solutions and particles.[60-64] For example, the World Health Organization has reported concentrations of 260 μg kg^{-1} in sewage sludge and up to 4.7 mg kg^{-1} in waste discharged from the jewelry industries.[65] Other sources of soluble palladium (often PdCl$_2$) such as e-waste (electroplating and printed circuit boards) can result in concentrations of 1500 mg L^{-1} in waste streams.[66] Concentrations in natural waters are significantly lower, with Pd concentrations of 22 ng L^{-1} and 70 pg L^{-1} being detected in fresh water and sea water, respectively.[67] Palladium metal has historically been considered relatively low in toxicity; however, its compounds such as palladium(II) chloride are highly toxic and carcinogenic to

wildlife even in minute amounts. For example, a minimum 24 h lethal concentration of 7 mg has been reported for the freshwater fish *medaka,* and LD$_{50}$ values in rats reach between 0.02 and 1.13 mmol kg^{-1} bodyweight;[67,68] hence, it is important to maximize recovery and clean waste already existing for both environmental and economic reasons.[4,67,69−71]

The primary method used to recover spent Pd catalysts is hydrometallurgy which is limited because of the significant volumes of toxic and expensive reagents needed and the further production of hazardous waste such as nitric oxides.[4,72−74] These methods, often requiring the pretreatment of Pd, have been able to achieve recovery within the range of 58−97%[75−83] but are considered ineffective for the removal of metals from waste solutions at low concentrations resulting in waste storage challenges and reduced profit.[66,84,85] Therefore, more environmentally sustainable methods of Pd nanoparticle synthesis and recovery have been investigated.[37,66,86,87] Electrodeposition is considered a practical method for metal recovery because of its operational feasibility, with the deposition controlled through the potential applied and metal ion concentration,[88−91] and traditional electrodeposition methods have many industrial applications.[92−98] The use of electrochemical systems such as galvanic reduction and recovery from ionic liquids after solvent extraction have been explored within the literature as a method of Pd extraction achieving a recovery of 90−99%.[66,99] Higher recoveries were observed in systems increasing mass transport via the use of rotating electrodes or flow of the plating solution.[100,101] However, overall recovery or recycling efficiency is not necessarily easily compared because studies often focus on one part of the recycling process (usually recovery, rather than separation, dissolution, etc.).

In this work, we consider the recovery process from solution: particle impact electrochemistry has been investigated as a method for in situ synthesis of Pd-modified carbon black nanoparticles (Pd/CB NPs) from the recovery of palladium from solutions containing low concentrations of PdCl$_2$ as a proxy for industrial waste streams.

The impact electrochemistry technique involves nanoparticles suspended in solution moving under Brownian motion and occasionally "colliding" with a substrate electrode held at a suitable potential.[102−105] While the particle-electrode interaction is usually referred to in terms of a "collision", there is of course no requirement for physical contact: provided the particle approaches sufficiently close to reach the plane of electron transfer (i.e., electron tunneling distance), then electroreduction or oxidation can occur. Upon collision, the nanoparticles provide a surface at which solution species can be oxidized or reduced,[106−123] resulting in transient current signals that can be analyzed to determine factors such as particle size, concentrations, and kinetics.[124−129] The shape of the transient signal can also be used to infer the type of collision (or interaction) between the particle and electrode, ranging from apparently fully elastic (rebound) impacts to fully inelastic ("hit and stick") impacts which appear to depend on a range of factors such as electrode and particle materials, surface groups, solution conditions, and so on. The extent of the electrochemical reaction occurring on the surface of the particle during a collision is therefore dependent on the conditions of the impact, most notably the electrochemical kinetics of the reaction and the duration of the particle-electrode "contact". Once the particle moves away from the

plane of electron transfer, no further (heterogeneous) electron transfer should occur. In some cases, the particles and substrate electrodes are chosen to be different materials: if the desired electrochemical reaction has significantly faster kinetics on the particle compared to the substrate, it is possible to only observe reactions at the particles. Where there is little or no difference in kinetics, the electrochemical reaction occurs at both the substrate and particles, which often makes observing impact signals challenging because of the respective current magnitudes.

Impact electrochemistry has previously been reported as a method of reducing metallic ions onto metallic nanoparticles (or cores) via both bulk and underpotential deposition processes.[130−132] However, the deposition onto nonmetallic cores (for metal recovery) via impact electrochemistry has only recently been described, for the deposition of copper ions onto fly-ash cenosphere particles.[133] The use of nonmetallic materials potentially increases the economic viability, flexibility, and sustainability of this technique as it reduces reliance on expensive and potentially critical core materials.

In this paper, we report the first metal on carbon deposition by impact electrochemistry for the case of Pd on CB, using the method to fabricate Pd/CB nanoparticles which were then characterized and directly used, as a proof of concept, to catalyze the hydrogen evolution and Suzuki coupling reactions. Under nonoptimized conditions, the fabrication process recovered >85% of Pd from solution in 26 h, suggesting the viability for this technique in recovery/recycling of metals.

2. EXPERIMENTAL SECTION

All chemicals used were obtained commercially and used without further purification, namely, palladium chloride (99.99%, Sigma-Aldrich), potassium chloride (99.0−100.5%, Alfa Aesar), potassium sulfate (99.0%, Alfa Aesar), sulfuric acid (95.0−98.0%, Sigma-Aldrich), hydrochloric acid (37.0%, Honeywell), and 50 nm-diameter CB nanoparticles (Fuel cell store). All solutions were made using ultrapure water of resistivity ≥18.2 MΩ cm (MilliQ, Millipore).

2.1. Electrochemistry. Electrochemical experiments were performed using a three-electrode cell in a Faraday cage. The working electrodes used were a glassy carbon macroelectrode (GC, 3 mm diameter, BASi Inc) and carbon fiber (CF) microelectrodes of diameters 33 μm (ALS Inc.) and 9 μm (made in-house using pitch-derived CF from Goodfellow Cambridge Ltd). All working electrodes were thoroughly polished with 3 μm diamond paste and alumina suspensions of 1, 0.3, and 0.05 μm sequentially, on a microcloth pad (all from Buehler Inc., USA). A saturated calomel electrode (SCE, ALS Inc) was used as a reference electrode and a graphite rod (3 mm diameter, Goodfellow Cambridge Ltd.) as the counter electrode. For impact studies, the SCE reference electrode was placed in a separate fritted compartment to prevent cross-contamination. Unless otherwise stated, a solution containing 0.01 M potassium chloride, 0.01 M hydrochloric acid, and 0.5 mM palladium(II) chloride was used. In this solution, the PdCl$_3^-$ ion is more prevalent than PdCl$_4^{2-}$ because of the relatively low chloride concentration (see the Supporting Information for calculation). A bulk solution of CB NPs was prepared by adding CB NPs to ultrapure water and sonicating for 1 h before use. The desired CB NP concentration of 50 pM was prepared using aliquots of the CB NP bulk solution. Solutions were thoroughly degassed using nitrogen gas (oxygen-free, BOC Gases plc), and a nitrogen atmosphere was maintained throughout the experiments. For impact experiments, the solution was bubbled with nitrogen regularly to agitate the particle suspension and inhibit aggregation. For particle-modified GC voltammetry, the GC electrode was prepared via a drop-cast method where 5 μL of the relevant NP suspension was added to a polished GC electrode surface and allowed to dry under nitrogen.

Standard electrochemical measurements were conducted using an Autolab 128 N (Metrohm-Autolab BV, Netherlands) potentiostat controlled via a PC running NOVA 2.1 software conducting both linear sweep voltammetry and chronoamperometry scans. Particle impact chronoamperometric scans were performed using a bespoke low noise potentiostat,[133] with a sampling rate of 100 kHz. All data were processed using a combination of Microsoft Excel and Origin Pro 2021. Unless stated otherwise, impact electrochemical data were analyzed following electronic filtration (digital) at 250 Hz in order to improve the signal-to-noise ratio and facilitate analysis. The design of the potentiostat is such that charge is conserved by the filter, as shown elsewhere.[133−135]

For the bulk synthesis of Pd-modified carbon nanoparticles (Pd/CB) using impact electrochemistry, a polished graphite plate working electrode (6.25 cm^2) with a larger area graphite counter electrode (Alfa Aesar) and a SCE reference electrode were used. Long-term chronoamperography (potential held at −0.1 V) was conducted in 500 mL of palladium solution with 20 nM 50 nm CB NPs to produce Pd/CB NP samples that had been modified for 168 h for imaging and testing for catalytic activity. The reacted Pd/CB samples were filtered using 0.02 μm anodisc membrane filters (Cytiva) and repeatedly rinsed with ultrapure water before drying. An analogous experiment was conducted for 24 h to fabricate Pd/CB nanoparticles which were tested electrocatalytically via the hydrogen evolution reaction (HER) by drop casting 5 μL (giving a catalyst mass of 8.5 g m^{-2}) onto a bare GC electrode.[133,136] To prepare the three catalyst inks, unmodified CB NPs, Pd/CB NPs (modified via impacts), and commercial 10% Pd on CB nanoparticles (Sigma-Aldrich) were added to ultrapure water respectively. This was followed by the addition of NafionTM dispersion D1021 (Fuel Cell Store) to each catalyst ink to achieve 10% of total mass (i.e., carbon plus Pd). Cyclic voltammetry (CV) scans were then conducted at 100 mV s^{-1} in a solution of 0.01 M H$_2$SO$_4$ and 0.09 M K$_2$SO$_4$ in the potential window of 1.0 to −1.7 V vs SCE using a graphite rod as the counter electrode.

To analyze the rate of Pd recovery, experiments were conducted for 26 h, as above, with and without the addition of CB NPs where the nitrogen flow rate was kept constant at 5 L min^{-1}, and 3 mL aliquots were extracted at designated time intervals. The samples were filtered and diluted with ultrapure water for inductively coupled plasma optical emission spectrometry (ICP-OES) using a PerkinElmer Optima 8000. A calibration curve was generated with a 10 ppm multielement calibration standard for ICP (Agilent), in ultrapure water at concentrations of 5−0.01 ppm. The samples were then analyzed, and the concentration of palladium was read from the calibration curve which has an upper concentration limit of 500 ppm.

2.2. Material Characterization of Pd-Modified CB NPs. Modified and unmodified CB nanoparticle samples were characterized using environmental scanning electron microscopy (ESEM) with energy-dispersive X-ray spectroscopy (EDX), transmission electron microscopy (TEM) with EDX, X-ray photoelectron spectroscopy (XPS) analysis, and inductively coupled plasma mass spectrometry (ICP-MS). For the ESEM/EDX characterization, 5 mg of CB nanoparticle samples were added to the surface of carbon tape (Agar Scientific) and then analyzed using a Philips XL30 FEG ESEM. For TEM, samples were drop-cast onto grids and imaged using a JEM-2100F Field Emission Electron Microscope operated at 200 kV, equipped with a Gatan Orius SC1000 CCD camera (performed at NMRC, University of Nottingham). HAADF-STEM data were acquired using JEOL DF detectors, and EDX data were acquired using an Oxford Instruments X-Max 80 EDX detector. For the XPS characterization, the samples were analyzed (at NMRC, University of Nottingham) using a Kratos Liquid Phase Photoelectron Spectrometer (LiPPS, in dry sample mode) with monochromated Al KαX-ray source (1486.6 eV). This was operated at 10 mA emission current and 12 kV anode potential (120 W). For the wide scan, a pass energy of 80 eV was used (run with a step size of 0.5 eV) while the high-resolution scan was conducted with a pass energy of 20 eV (with a step size of 0.1 eV). Data processing was conducted using CASAXPS software (version 2.3.20) with Kratos sensitivity factors (RSFs) to determine the atomic percentage values from the peaks.

For the ICP-MS analysis, three samples were dissolved in aqua regia, then diluted using ultrapure water to obtain 1% aqua regia at a concentration of 1 ppm (CB content), and filtered with 0.45 μm syringe filters (Starlab Group Ltd). The samples were then analyzed using ICP-MS (Nexion 300X ICP-MS, PerkinElmer) with a limit of detection of 10 ppt. A calibration curve was generated as described for the ICP-OES analysis ranging from 1 ppb to 1 ppm.

Thermogravimetric analysis (TGA) (sample weight 8.61 mg) was performed using NETZSCH TG 209 F1 in an aluminum oxide crucible at a heating rate of 10 °C min^{-1} from 25 to 900 °C under nitrogen purging (10 mL min^{-1}), and sample weights were additionally measured using the nanobalance (Sartorius) before and after thermal treatment.

2.3. Catalysis of the Suzuki Coupling Reaction. For the Suzuki coupling reaction, a solution of 184 mg of phenylboronic acid (≥97.0%, Sigma-Aldrich), 426 mg of potassium phosphate tribasic (≥ 98.0%, Sigma-Aldrich), and 20 mL of ultrapure water was added to a three-necked round bottom flask and stirred (450 rpm) for 20 min. To this mixture 115 μL of iodobenzene (98.0%, Sigma-Aldrich) and ca. 30 mg of Pd-modified carbon nanoparticles were added while stirring. The mixture was stirred and refluxed in a silicone oil bath at 80 °C for 6 h. After cooling, the organic phase was extracted three times using 20 mL of ethyl acetate (Sigma-Aldrich) and then dried using anhydrous sodium sulfate (Sigma-Aldrich). The sodium sulfate was removed from the organic phase using 5−13 μm filter paper (Fisherbrand), and then the ethyl acetate was evaporated. The powdered sample was dissolved in CDCl$_3$ for ^{1}H NMR analysis using a Bruker 400 MHz NMR spectrometer where four scans were conducted with an acquisition time of 4.7 s and relaxation delay of 2 s. Data were analyzed using Mestrenova software (version 14.0.0).

3. RESULTS AND DISCUSSION

3.1. Impact Deposition of Pd onto CB Nanoparticles. First, preliminary experiments were performed to confirm the deposition of Pd onto carbon surfaces and to determine at which potentials the deposition onto CB NPs during impacts might occur. To do this, the deposition of Pd from a solution containing 0.5 mM PdCl$_2$, 0.01 M KCl, and 0.01 M HCl was investigated using macroelectrode CV at a voltage scan rate of 100 mV s^{-1} to determine the onset potential on the bare GC electrode, where onset is defined here as the potential at which the measured current density was −0.5 mA m^{-2}.[137−139]

Figure 1 shows the reductive segments of CV scans showing the deposition of palladium on the surface of 3 mm bare GC
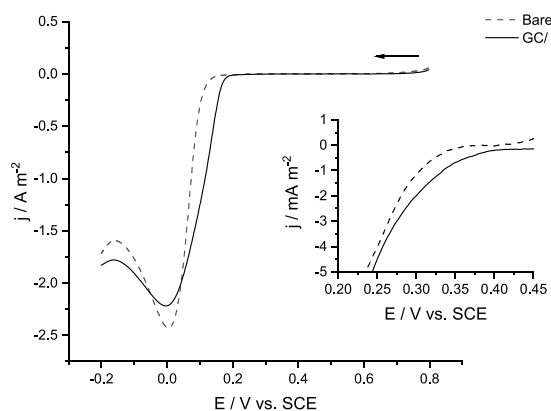

Figure 1. Reductive voltammetric scans of Pd deposition from a solution of 0.5 mM PdCl$_2$, 0.01 M KCl, and 0.01 M HCl onto the surface of 3 mm bare GC (·····) and 50 nm CB NP-modified GC (—) electrode where the inset shows the magnified onset potentials where Pd deposition commences. The voltage scan rate was 100 mV s^{-1} for all scans.
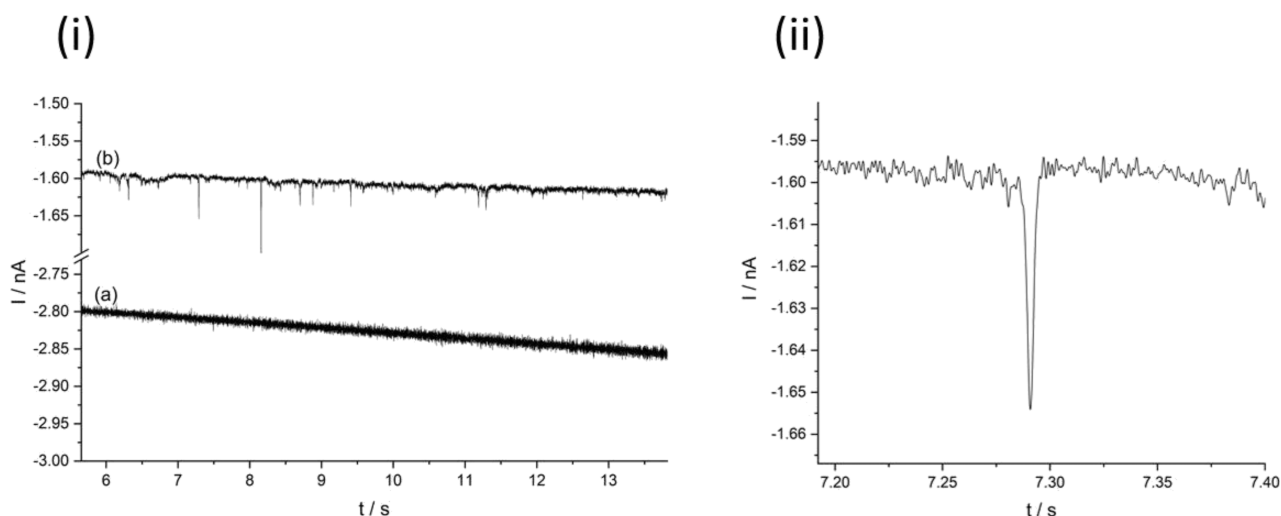
Figure 2. (i) Typical segments of chronoamperometric scans conducted at −0.1 V vs SCE using a 9 μm CF electrode: (a) before and (b) after the addition of 50 pM 50 nm CB nanoparticles to a solution of 0.5 mM PdCl$_2$, 0.01 M KCl, and 0.01 M HCl. (ii) A magnified reductive signal from scan (b) at t = 7.29 s.

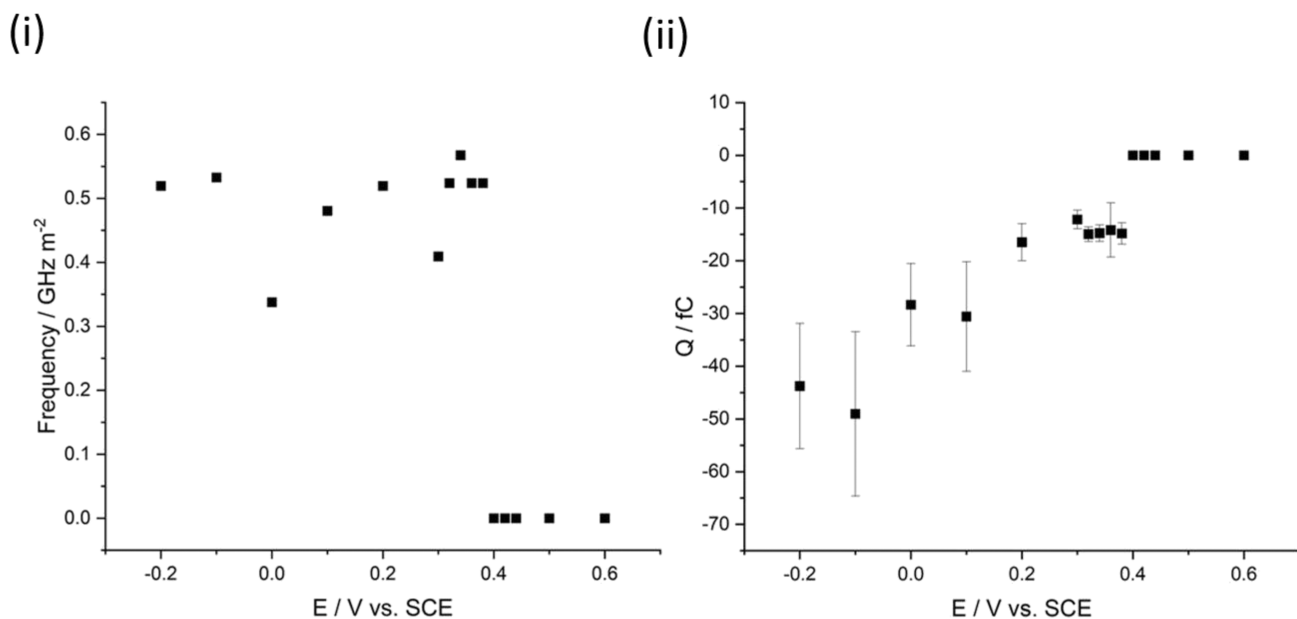**Figure 3.** (i) shows the frequency of reductive transient peaks detected during 30 s chronoamperometric scans at different potentials ranging from +0.6 to −0.2 V vs SCE using both 33 and 9 μm CF electrodes and (ii) displays the mean calculated charge passed during transient deposition events analyzed using unfiltered peaks. All scans were conducted in a 5 mL solution of 0.5 mM PdCl$_2$, 0.01 M KCl, and 0.01 M HCl.

and 50 nm carbon black-modified GC electrodes. The CB-modified GC electrode was prepared via a drop-cast method where 5 μL of the CB NP suspension was added to a polished GC electrode surface and allowed to dry, resulting in a surface (particle) concentration of 66 pmol m^{-2}. The deposition of palladium is known to be a two-electron transfer,[46,54]

$$Pd^{2+}_{(aq)} + 2e^- \rightarrow Pd_{(s)},$$ where the nucleation mechanism and morphology of the deposited Pd are influenced by deposition conditions such as applied potential and Pd concentration.[88] The literature records the bulk deposition process to occur at potentials lower than *ca.* +0.3 to +0.4 V (vs SCE) depending on the carbonaceous material.[88,140] This is in good agreement with the recorded data (Figure 1) showing the onset at +0.29 V (vs SCE) for the bare GC and +0.38 V (vs SCE) on the CB NP-modified GC. The proximity of these onset potentials suggests that it is unlikely that Pd will deposit onto CB NPs

during impacts without some degree of background deposition onto the substrate GC electrode. It has previously been shown that at more positive potentials (lower overpotential) the electronucleation of Pd occurs via a 3D instantaneous mechanism while more negative potentials (higher over-potential) result in a 3D progressive nucleation mechanism.[88,141,142]

Having determined the onset potentials for Pd deposition on GC and CB NPs under these conditions, chronoamperometric scans were conducted in the presence and absence of nanoparticles to investigate whether transient impact events occurred. The chronoamperometric scans were conducted using a three-electrode cell in a 0.5 mM palladium solution (as described previously) where either a 9 μm or a 33 μm diameter CF electrode acted as the substrate surface.
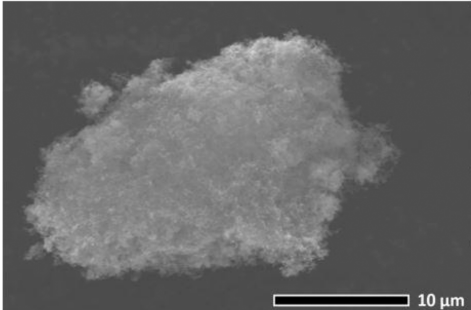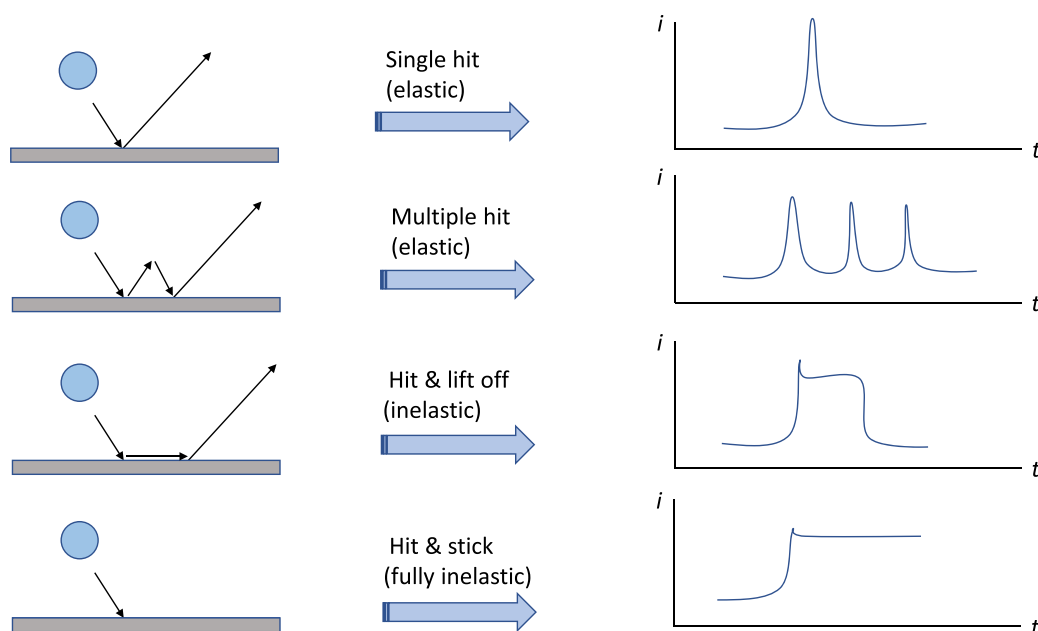
Figure 4. Schematic showing some possible impact scenarios and simplified transient signals.

Table 1. SEM Image of Agglomerated CBNPs Obtained from a 24 h Chronoamperometric Scan Conducted at −0.1 V (vs SCE) in a Solution of 0.5 mM $PdCl_2$, 0.01 M KCl, and 0.01 M HCl[a]

	CBNP samples	SEM/ EDX average weight% ratio Pd/CB	ICP-MS Pd conc. (ppm)
	unmodified	0	0.01[b]
	0.6V vs SCE	0.03 ± 0.005	2.75
	-0.1V vs SCE	0.09 ± 0.009	17.67

[a]The table displays palladium content determined by SEM/ EDX and ICP-MS analysis of the unmodified CBNPs, the sample held at +0.6 V vs SCE during chronoamperometry, and the sample held at −0.1 V vs SCE. [b]Measurement equivalent to zero within error.

Figure 2 displays two chronoamperometric scans conducted using a 9 μm CF microelectrode at −0.1 V vs SCE before (a) and after (b) the addition of CB nanoparticles where scan (a) is void of reductive peaks. Upon the addition of nanoparticles, peaks were observed indicating the deposition of palladium onto the CB NPs upon impact. At this potential, Pd deposition may occur at CB NPs as well as the substrate GC electrode (see Figure 1), and so the measured currents reflect the capacitance of the GC substrate as well as any faradaic currents because of Pd deposition. The difference in currents of (a) and (b) is ascribed to fluctuations because of natural convection given the length of each chronoamperometric scan. Impact studies were conducted on both 9 and 33 μm CF electrodes: the former was used predominantly for potentials close to the onset of deposition, where transient signals were small, and optimal signal-to-noise ratios were required. Although the smaller electrode provided lower noise levels due to lower capacitance (see Supporting Information Section A), its smaller area also led to less frequent transient signals, and hence for convenience, the larger CF substrate electrodes were used at potentials further from onset to provide a greater quantity of data more rapidly.

Further impact studies were conducted by performing multiple chronoamperometric scans using 50 pM CB NPs at potentials between +0.6 and −0.2 V vs SCE. The impact frequency was determined at each potential by dividing the total number of observed impact signals by the total time of all scans, as seen in Figure 3i and was in the range of 0.34−0.57 GHz m^{-2} (within the literature a frequency range of 0.7−3.7 GHz m^{-2} is documented for metal deposition impacts using ca. 20 pM metallic cores.[130,133]). From Figure 3, reductive peaks can be observed at potentials negative of +0.4 V vs SCE, consistent with the onset observed in Figure 1. At all potentials, the impact signals had a similar duration, indicating that deposition of Pd occurred during approximately elastic collisions with the electrode (if deposition occurred at NPs that had preadsorbed to the GC surface, then step-like signals would be observed, see Figure 4 for a schematic). The role of preadsorbed Pd^{2+} is less straightforward to quantify and may well prove to be key to electrodeposition during impacts, especially where reduction kinetics may be less than reversible.

Integration of the CB NP reductive transients produced the charge associated with Pd deposition on individual nanoparticles (see Supporting Information Section B Table T1).[133]

Figure 3ii shows the average charge of impacting CB NPs at different potentials ranging from +0.6 to −0.2 V vs SCE where at potentials more reductive than +0.4 V, charge ranging from −12.2 to −49.0 fC is observed, seemingly increasing with increased overpotential. The theoretical Pd coverage can be calculated based on the charge transferred during impacts (see Supporting Information Section B for details). For example, at +0.38 V (vs SCE) an average charge of −14.8 ± 2.1 fC corresponds to a coverage of 110 ± 15%, increasing to 365 ± 116% at a more reductive potential of −0.1 V (vs SCE) where the charge was −49.0 ± 15.6 fC.

3.2. Characterization of Pd-Modified CB NPs. To confirm palladium deposition on the CB nanoparticles, a 24 h impact experiment was conducted using a graphite plate electrode (area 6.25 cm^2) held at a potential of −0.1 V (vs SCE) in 500 mL of a solution containing 0.5 mM PdCl$_2$, 0.01 M KCl, and 0.01 M HCl. The upscaling of the experiment was required to produce sufficient mass of impacted CB NPs to analyze. A concentration of 20 nM CB NPs was added to the solution and agitated continually with a nitrogen gas stream for the 24 h period. An analogous experiment was conducted at +0.6 V vs SCE, where no transient impact peaks due to Pd reduction were expected. The two samples held at −0.1 V and +0.6 V were rinsed thoroughly with deionized water during filtration using 0.02 μm anodisc inorganic membrane filters before drying.

The samples in addition to unmodified CB NPs were characterized using ESEM/EDX and ICP-MS with results shown in Table 1. The ESEM/EDX analysis indicated that no palladium was detected in the unmodified sample, as expected as it had not been in contact with the PdCl$_2$ solution. The sample held at −0.1 V exhibited the highest average weight % ratio Pd/C of 0.09 ± 0.009 followed by the sample held at +0.6 V with an average weight % ratio Pd/C of 0.03 ± 0.005. Analysis by ICP-MS showed a similar trend with the measured Pd concentration of 0.01, 2.75, and 17.67 ppm for the samples of unmodified CBNPs, held at 0.6 V vs SCE during chronoamperometry and at −0.1 V vs SCE, respectively. The Pd detected in the sample held at +0.6 V reflects the residual trace adsorbed palladium(II) left after the washing procedure. This level of Pd(II) appears to remain regardless of the extent of washing, suggesting adsorption to the CB surface, possibly via oxygen moieties. To further analyze the samples and determine the oxidation state of the Pd detected, XPS analysis was conducted on +0.6 and −0.1 V modified samples, shown in Figure 5. The data suggest that trace palladium was detected on the unmodified sample similar to results determined by the ESEM/EDX and ICP-MS analysis.

The Pd 3d XPS characterization of the sample held at −0.1 V vs SCE indicated the presence of both Pd^0 and Pd^{2+}, with the latter associated with both PdCl$_2$ and PdO. The peak with a lower binding energy (Pd 3d$_{5/2}$) of 335.49 eV is assigned to the metallic palladium (Pd^0) content while the peaks with a binding energy of 336.14 and 338.10 eV indicate the presence of PdO and PdCl$_2$ respectively.[143−150] The presence of Pd^0 suggests that during impact events the potential was sufficiently negative to facilitate the reduction of Pd^{2+} to Pd^0, which may have later (partially) oxidized to form PdO. Analysis of the sample held at +0.6 V vs SCE demonstrated the presence of Pd^{2+} as PdCl$_2$ (with binding energies 337.94 and 343.96 eV) but no Pd^0. This supports the earlier conclusion from the ESEM/EDX and ICP-MS data that some residual PdCl$_2$
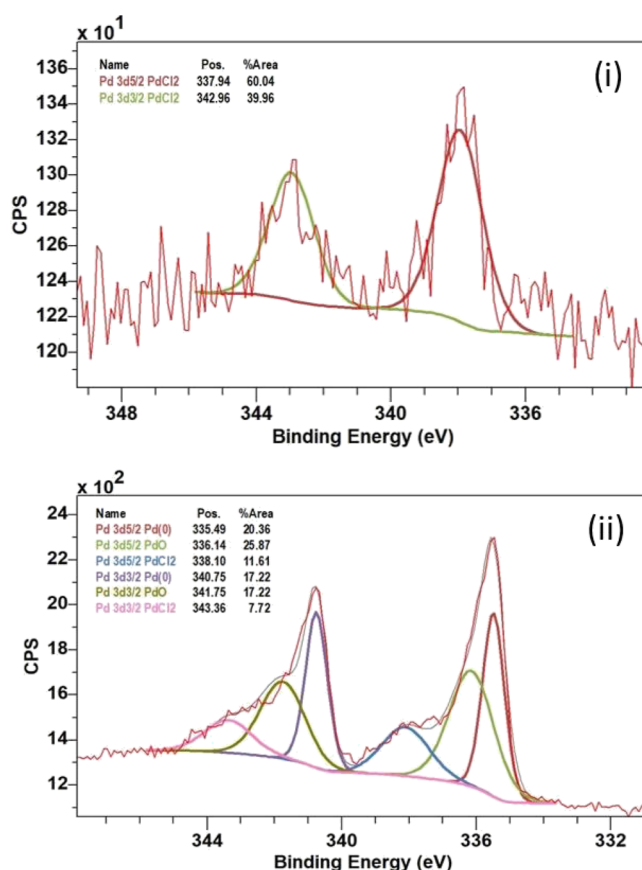

Figure 5. XPS spectra (Pd 3d$_{5/2}$ and Pd 3d$_{3/2}$) of (i) +0.6 V vs SCE modified CB NPs and (ii) −0.1 V vs SCE modified CB NPs where the peaks with a binding energy of 335.49 eV (Pd 3d$_{5/2}$) and 340.75 eV (Pd 3d$_{3/2}$) indicate Pd^0.

persisted after washing and no palladium deposition had occurred during collision at +0.6 V vs SCE.

3.3. Synthesis and Testing of Pd/CB NP Catalysts. To sufficiently scale-up the quantity of Pd/CB NPs fabricated for testing in the hydrogen evolution and Suzuki coupling reactions, a batch of Pd/CB NPs was produced from a longer-term, 24 h, and 168 h deposition experiment (see the Experimental Section). Subsequent analysis by TGA (see Supporting Information Section C Figure S2) suggested that the Pd/CB NPs contained 14% by mass of Pd. The TEM images (Figure 6i−vi) further highlighted the presence of palladium metal on some particles evident in the contrasting darker regions seen on the carbon core, confirmed with EDX mapping (see Supporting Information Section D Figure S3). Deposition did not occur consistently across all Pd/CB NPs as some CB NPs were void of Pd suggesting that not all CBNPs collided with the GC electrode during the investigation or alternatively some collisions resulted in little to no Pd deposition. Figure 6 (TEM images of the impacted particles) suggests that the Pd deposits formed were not singular nanoparticles evenly distributed across the surface of the CB particles, but rather deposits covering sections of the impacting particle. Using the tilt function of the TEM, it was observed that these growths followed the curvature of the carbon particle rather than directly protruding out from the particle surface (Figure 6vi), and future work will explore further details of the Pd deposition to shed light on the mechanism of metal deposition during impact.
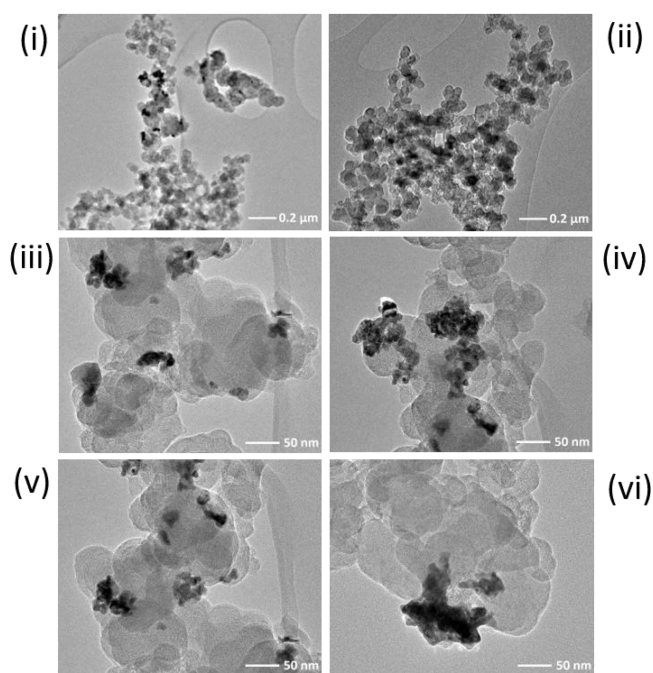
F

Figure 6. Typical TEM images (i–vi) of the 168 h palladium-modified carbon nanoparticles where the darker regions represent deposited Pd metal.

As a simple test of the catalytic capabilities of the Pd/CB NPs as catalysts without further treatment, samples were used for both hydrogen evolution and Suzuki coupling reactions. For the HER, 24 h modified Pd/CB NPs were compared with commercial 10 wt % Pd on CB catalyst. The test was conducted in a solution of 0.01 M H_2SO_4 and 0.09 M K_2SO_4 and showed the characteristic proton reduction profile for both the commercial standard and the impact synthesized sample (see Supporting Information Section E).

For the Suzuki reaction, 30 mg of 168 h modified Pd/CB NPs was used to catalyze the reaction between benzeneboronic acid (phenylboronic acid), iodobenzene, and potassium phosphate to produce biphenyl.[16,17,37] This was achieved under 80 °C reflux where the resulting product was identified using ^{1}H NMR. It should be noted that the quantity of Pd/CB NPs used is not optimized: at 14 wt % Pd this quantity of NPs provides *ca.* 4.2 mg of Pd, chosen to produce sufficient product for convenient handling and analysis.[37] It was determined that the Pd/CB NPs had successfully catalyzed the reaction producing a mixture of biphenyl and residual benzeneboronic acid, evidenced by ^{1}H NMR spectra of the product mixture (Figure 7i, spectrum (c)) which indicated that the iodobenzene had reacted and was no longer present in the final product as the signals at 7.10 ppm (spectrum (a)) are no longer observed. The multiplets at 7.60, 7.45, and 7.35 ppm in both the reference spectrum (b) and the product spectrum (c) suggest the presence of biphenyl. The additional signals can be attributed to the excess benzeneboronic acid initially used in the reaction.

3.4. Palladium Recovery from Low Concentration of PdCl₂. Finally, the use of the impact method as a means to recover Pd from solution was studied. To examine the change in $PdCl_2$ concentration during the impact deposition process, and hence Pd recovery from solution, 26 h chronoamperometric scans were conducted with and without CBNPs where a flow rate of nitrogen at 5 L min^{-1} (selected due to the range of
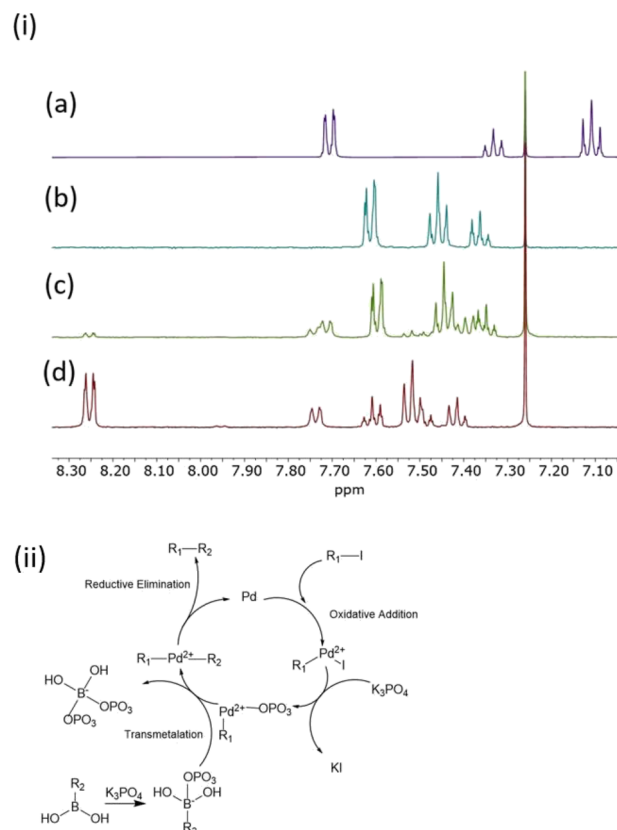

Figure 7. (i) ^{1}H NMR spectrum of (a) iodobenzene, (b) biphenyl product taken from doi:10.13018/BMSE000506,[151,152] (c) product extracted during the Suzuki reaction using Pd/CB NPs, and (d) displaying the ^{1}H NMR analysis of the benzeneboronic acid reactant used in the investigation. The ^{1}H NMR was performed using $CDCl_3$ identified by the singlet at 7.26 ppm and (ii) schematic of the Suzuki reaction mechanism.

flow rate gauges available) was maintained to ensure the same level of agitation. A 500 mL solution containing 0.01 M potassium chloride, 0.01 M hydrochloric acid, and 0.4 mM palladium(II) chloride (determined by ICP-OES) was used. The lower initial concentration determined by ICP-OES may be due to the presence of high levels of potassium ions in the samples causing a suppression of the Pd signal.[153,154] At regular intervals throughout the experiments, 3 mL aliquots were extracted and filtered with 0.45 μm syringe filters to prepare samples for ICP-OES analysis.

Figure 8i shows the percentage of Pd^{2+} recovered during a 26 h chronoamperometric scan with and without the addition of CB NPs. Figure 8ii shows the depletion in Pd^{2+} concentration in logarithmic form: the NP-mediated experiment showing an enhancement in the recovery rate of a factor of approximately 1.7, for these nonoptimized conditions. Despite each individual nanoimpact resulting in the deposition of *ca.* 10^5 Pd atoms, the high number of impacts has a significant effect on the overall rate of removal of Pd from solution. Future work will seek to quantify the relationship between the experimental parameters and recovery rate.

The background deposition occurring on the graphite substrate electrode during chronoamperometric scans with and without CB NPs was studied via ESEM/EDX (see Supporting Information Section F). A comparison of Figure S6 displaying a polished graphite electrode with Figures S7 and S8 showing an electrode held in solution under potential for as
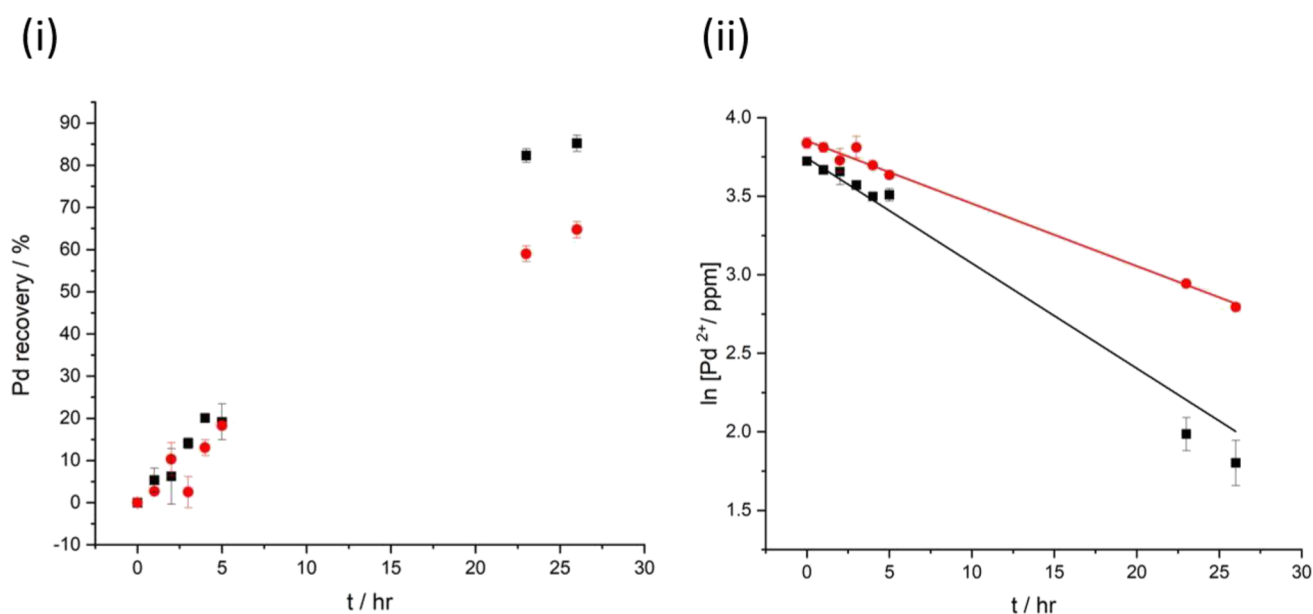
Figure 8. (i) Percentage of Pd recovered from $PdCl_2$ during a 26 h chronoamperometric scan conducted with (black square ■) and without (red circle ●) CB NP particles. (ii) $\ln[Pd^{2+}]$ vs time based on the data in (i) where the best fit lines from linear regression are given by $\ln[Pd^{2+}/ppm] = 3.74 - 0.067\,t$ for (black square ■) and $\ln[Pd^{2+}/ppm] = 3.85 - 0.04\,t$ for (red circle ●).

long as 168 h confirms that Pd deposition occurs on the electrode resulting in a heavily modified surface. Figure S9 shows a side profile of both graphite electrodes (modified with and without CBNPs) indicating that the extent of Pd deposition on the background electrode is more prominent without the presence of particles. An average Pd thickness of 2.2 μm with larger growths (some exceeding 10 μm) was seen on the electrode without CBNPs in comparison to an average thickness of 0.5 μm seen on the electrode used with CB NPs present.

4. CONCLUSIONS

Initial deposition studies conducted on glassy carbon showed that bulk deposition of Pd occurred at potentials negative of *ca.* +0.4 V (vs SCE), in good agreement with the literature.[88,140,142] Subsequent impact electrochemistry studies with CB NPs showed that transient impact events resulting in Pd deposition also commenced at *ca.* +0.40 V (vs SCE). Analysis of the resulting transient peaks determined an average charge of -14.8 ± 2.1 fC was observed at the "switch on/off potential" of +0.38 V (vs SCE) increasing to -49.0 ± 15.6 fC at a potential of -0.1 V (vs SCE).

Direct evidence of impact-mediated Pd deposition on the CB NPs was obtained via ESEM, EDX, TEM, ICP-MS, and XPS analysis of the Pd/CB NP sample. The impact experiment was successfully scaled up to produce enough Pd/CB NPs to test as a catalyst through large-volume long-term chronoamperometry, and synthesized Pd/CB NPs were characterized using TEM and TGA confirming a metal loading of 14 wt % Pd. The particles were then used to demonstrate direct catalytic application via the hydrogen evolution and Suzuki coupling reactions.

Finally, Pd recovery via nanoimpacts was investigated. Although not optimized to recover the maximum amount of Pd from solution, it was found that comparing Pd recovery with and without CB NPs over a 26-h period, the NP-mediated method increased recovery from *ca.* 65% to *ca.* 85%. This demonstrates the potential for single-entity electrochemistry to

be a useful recovery method for metals, and future work will investigate its optimization and develop semiempirical equations for practical use as well as exploring applications for the deposited metal such as using 3D structured substrate electrodes that could be used for energy storage (e.g., recovered Ni, Mn, and Co for battery materials).

■ ASSOCIATED CONTENT

ⓢ Supporting Information

The Supporting Information is available free of charge at https://pubs.acs.org/doi/10.1021/jacs.2c08239.

> Transient current signal analysis using 9 and 33 μm CF; reductive peak charge and coverage analysis; TGA of the 168 h modified Pd/CB NP sample; TEM/EDX of impacted CB NPs; LSV of HER using modified CB NPs; cleaning CV conducted before HER investigation; and ESEM/EDX of the electrode used in Pd recovery investigation (PDF)

■ AUTHOR INFORMATION

Corresponding Author

Neil V. Rees − *School of Chemical Engineering, University of Birmingham, Birmingham B15 2TT, U. K.;* ⓞ orcid.org/0000-0002-5721-1453; Email: n.rees@bham.ac.uk

Authors

Abiola V. Oladeji − *School of Chemical Engineering, University of Birmingham, Birmingham B15 2TT, U. K.*

James M. Courtney − *School of Chemical Engineering, University of Birmingham, Birmingham B15 2TT, U. K.*

Marcos Fernandez-Villamarin − *School of Chemical Engineering, University of Birmingham, Birmingham B15 2TT, U. K.*

Complete contact information is available at:
https://pubs.acs.org/10.1021/jacs.2c08239

◼ ABBREVIATIONS

PGM	platinum group metals
CB NPs	carbon black nanoparticles
SCE	saturated calomel electrode
CV	cyclic voltammetry
LSV	linear sweep voltammetry
GC	glassy carbon
CF	carbon fiber
ESEM	environmental scanning electron microscopy
EDX	energy-dispersive X-ray spectroscopy
TEM	transmission electron microscopy
XPS	X-ray photoelectron spectroscopy
ICP-MS	inductively coupled plasma mass spectrometry
ICP-OES	inductively coupled plasma optical emission spectrometry

◼ REFERENCES

(1) Nose, K.; Okabe, T. H. Platinum Group Metals Production. In *Treatise on Process Metallurgy*; Elsevier, 2014; pp. 1071−1097.

(2) Hughes, A. E.; Haque, N.; Northey, S. A.; Giddey, S. Platinum Group Metals: A Review of Resources, Production and Usage with a Focus on Catalysts. *Resources* **2021**, *10*, 93.

(3) Crundwell, F. K.; Moats, M. S.; Ramachandran, V.; Robinson, T. G.; Davenport, W. G. Platinum-Group Metals, Production, Use and Extraction Costs. In *Extractive Metallurgy of Nickel, Cobalt and Platinum Group Metals*; Elsevier; 2011; pp. 395−409.

(4) Jamali, M. R.; Assadi, Y.; Kozani, R. R. Determination of Trace Amounts of Palladium in Water Samples by Graphite Furnace Atomic Absorption Spectrometry after Dispersive Liquid-Liquid Micro-extraction. *J. Chem.* **2012**, *2013*, No. 671743.

(5) Antolini, E. Palladium in Fuel Cell Catalysis. *Energy Environ. Sci.* **2009**, *2*, 915−931.

(6) Kumar, S. S.; Ramakrishna, S. U. B.; Devi, B. R.; Himabindu, V. Phosphorus-doped carbon nanoparticles supported palladium electro-catalyst for the hydrogen evolution reaction (HER) in PEM water electrolysis. *Ionics* **2018**, *24*, 3113−3121.

(7) Huang, Y. -X.; Liu, X. -W.; Sun, X. -F.; Sheng, G. -P.; Zhang, Y. -Y.; Yan, G. -M.; Wang, S. -G.; Xu, A. -W.; Yu, H. -Q. A new cathodic electrode deposit with palladium nanoparticles for cost-effective hydrogen production in a microbial electrolysis cell. *Int. J. Hydrogen Energy* **2011**, *36*, 2773−2776.

(8) Alexeyeva, N.; Sarapuu, A.; Tammeveski, K.; Vidal-Iglesias, F. J.; Solla-Gullón, J.; Feliu, J. M. Electroreduction of Oxygen on Vulcan Carbon Supported Pd Nanoparticles and Pd−M Nanoalloys in Acid and Alkaline Solutions. *Electrochim. Acta* **2011**, *56*, 6702−6708.

(9) Seo, M. H.; Choi, S. M.; Lee, D. U.; Kim, W. B.; Chen, Z. Correlation Between Theoretical Descriptor and Catalytic Oxygen Reduction Activity of Graphene Supported Palladium and Palladium Alloy Electrocatalysts. *J. Power Sources* **2015**, *300*, 1−9.

(10) Safavi, A.; Kazemi, S. H.; Kazemi, H. Electrocatalytic Behaviors of Silver−Palladium Nanoalloys Modified Carbon Ionic Liquid Electrode Towards Hydrogen Evolution Reaction. *Fuel* **2014**, *118*, 156−162.

(11) Shao, M. Palladium-based Electrocatalysts for Hydrogen Oxidation and Oxygen Reduction Reactions. *J. Power Sources* **2011**, *196*, 2433−2444.

(12) Limpattayanate, S.; Hunsom, M. Electrocatalytic Activity of Pt−Pd Electrocatalysts for The Oxygen Reduction Reaction in Proton Exchange Membrane Fuel Cells: Effect of Supports. *Renewable Energy* **2014**, *63*, 205−211.

(13) Sarkar, S.; Peter, S. C. An Overview on Pd-Based Electro-catalysts for The Hydrogen Evolution Reaction. *Inorg. Chem. Front.* **2018**, *5*, 2060−2080.

(14) Katara, P. Review Paper on Catalytic Converter for Automobile Exhaust Emission. *Int. J. Sci. Res.* **2016**, *5*, 30−33.

(15) Roy, K.; Jain, R.; Ghosalya, M. K.; Reddy, K. P.; Gopinath, C. S. Three-Way Catalytic Converter Reactions Aspects at Near-Ambient Temperatures on Modified Pd-Surfaces. *C. R. Chim.* **2016**, *19*, 1363−1369.

(16) Wolfe, J. P.; Singer, R. A.; Yang, B. H.; Buchwald, S. L. Highly Active Palladium Catalysts for Suzuki Coupling Reactions. *J. Am. Chem. Soc.* **1999**, *121*, 9550−9561.

(17) Li, Z.; Bucbaum, C.; Heaner, W. L., IV; Fisk, J.; Jaganathan, A.; Holden, B.; Pollet, P.; Liotta, C. L. Palladium-Catalyzed Suzuki Reactions in Water with No Added Ligand: Effects of Reaction Scale, Temperature, pH of Aqueous Phase, and Substrate Structure. *Org. Process Res. Dev.* **2016**, *20*, 1489−1499.

(18) Miyaura, N.; Suzuki, A. Palladium-Catalyzed Cross-Coupling Reactions of Organoboron Compounds. *Chem. Rev.* **1995**, *95*, 2457−2483.

(19) Suzuki, A. Recent Advances in The Cross-Coupling Reactions of Organoboron Derivatives with Organic Electrophiles, 1995−1998. *J. Organomet. Chem.* **1999**, *576*, 147−168.

(20) Kotha, S.; Lahiri, K.; Kashinath, D. Recent Applications of the Suzuki−Miyaura Cross-coupling Reaction in Organic synthesis. *Tetrahedron* **2002**, *58*, 9633−9695.

(21) Bellina, F.; Carpita, A.; Rossi, R. Palladium Catalysts for the Suzuki Cross-Coupling Reaction: An Overview of Recent Advances. *Synthesis* **2004**, *2004*, 2419−2440.

(22) Magano, J.; Dunetz, J. R. Large-Scale Applications of Transition Metal-Catalyzed Couplings for the Synthesis of Pharmaceuticals. *Chem. Rev.* **2011**, *111*, 2177−2250.

(23) Nasrollahzadeh, M.; Sajadi, S. M.; Maham, M. Green Synthesis of Palladium Nanoparticles Using Hippophae Rhamnoides Linn Leaf Extract and Their Catalytic Activity for The Suzuki−Miyaura Coupling in Water. *J. Mol. Catal. A: Chem.* **2015**, *396*, 297−303.

(24) Siddiqi, K. S.; Husen, A. Green Synthesis, Characterization and Uses of Palladium/Platinum Nanoparticles. *Nanoscale Res. Lett.* **2016**, *11*, 482.

(25) Mandali, P. K.; Chand, D. K. Palladium Nanoparticles Catalyzed Suzuki Cross-Coupling Reactions in Ambient Conditions. *Catal. Commun.* **2013**, *31*, 16−20.

(26) Heugebaert, T. S. A.; De Corte, S.; Sabbe, T.; Hennebel, T.; Verstraete, W.; Boon, N.; Stevens, C. V. Biodeposited Pd/Au bimetallic nanoparticles as novel Suzuki catalysts. *Tetrahedron Lett.* **2012**, *53*, 1410−1412.

(27) Peng, Y.-Y.; Liu, J.; Leia, X.; Yina, Z. Room-temperature highly efficient Suzuki−Miyaura reactions in water in the presence of Stilbazo. *Green. Chem* **2010**, *12*, 1072−1075.

(28) Blakemore, D. C. Suzuki−Miyaura Coupling. In *Synthetic Methods in Drug Discovery: Volume 1*; Royal Society of Chemistry, 2015; pp. 1−69.

(29) Oosthuizen, R. S.; Nyamori, V. O. Carbon Nanotubes as Supports for Palladium and Bimetallic Catalysts for Use in Hydrogenation Reactions. *Platinum Met. Rev.* **2011**, *55*, 154−169.

(30) Fuentes, A. S.; Filippin, A. F.; Aguirre, M. D. C. Pd Nucleation and Growth Mechanism Deposited on Different Substrates. *Procedia Mater. Sci.* **2015**, *8*, 541−550.

(31) Singh, S. B.; Tandon, P. K. Catalysis: A Brief Review on Nano-Catalyst. *J. Energy Chem. Eng.* **2014**, *2*, 106−115.

(32) Mahesh, K. N.; Balaji, R.; Dhathathreyan, K. S. Palladium Nanoparticles as Hydrogen Evolution Reaction (HER) Electrocatalyst in Electrochemical Methanol Reformer. *Int. J. Hydrogen Energy* **2016**, *41*, 46−51.

(33) Long, N. V.; Hien, T. D.; Asaka, T.; Ohtaki, M.; Nogami, M. Synthesis and Characterization of Pt-Pd Alloy and Core-Shell Bimetallic Nanoparticles for Direct Methanol Fuel Cells (DMFCS): Enhanced Electrocatalytic Properties of Well-Shaped Core-Shell Morphologies And Nanostructures. *Int. J. Hydrogen Energy* **2011**, *36*, 8478−8491.

(34) Schlögl, R.; Abd Hamid, S. B. Nanocatalysis: Mature Science Revisited or Something Really New? *Angew. Chem., Int. Ed.* **2004**, *43*, 1628−1637.

(35) Prinsen, P.; Luque, R. Chapter 1. Introduction to Nano-catalysts. In *Nanoparticle Design and Characterization for Catalytic Applications in Sustainable Chemistry*; Royal Society of Chemistry, 2019; pp. 1−36.

(36) Li, Z.; Li, M.; Bian, Z.; Kathiraser, Y.; Kawi, S. Design of Highly Stable and Selective Core/Yolk−Shell Nanocatalysts—A Review. *Appl. Catal. B* **2016**, *188*, 324−341.

(37) Khan, M.; Albalawi, G. H.; Shaik, M. R.; Khan, M.; Adil, S. F.; Kuniyil, M.; Alkhathlan, H. Z.; Al-Warthan, A.; Siddiqui, M. R. H. Miswak Mediated Green Synthesized Palladium Nanoparticles as Effective Catalysts for The Suzuki Coupling Reactions in Aqueous Media. *J. Saudi Chem. Soc.* **2017**, *21*, 450−457.

(38) Wang, X. X.; Tan, Z. H.; Zeng, M.; Wang, J. N. Carbon Nanocages: A New Support Material for Pt Catalyst with Remarkably High Durability. *Sci. Rep.* **2014**, *4*, 4437.

(39) Su, D. S.; Centi, G. A. Perspective on Carbon Materials for Future Energy Application. *J. Energy Chem.* **2013**, *22*, 151−173.

(40) Pushkarev, A. S.; Pushkareva, I. V.; Grigoriev, S. A.; Kalinichenko, V. N.; Presniakov, M. Y.; Fateev, V. N. Electrocatalytic Layers Modified by Reduced Graphene Oxide for PEM Fuel Cells. *Int. J. Hydrogen Energy* **2015**, *40*, 14492−14497.

(41) Ramakrishna, S. U. B.; Reddy, D. S.; Kumar, S. S.; Himabindu, V. Nitrogen Doped CNTs Supported Palladium Electrocatalyst for Hydrogen Evolution Reaction in PEM Water Electrolyser. *Int. J. Hydrogen Energy* **2016**, *41*, 20447−20454.

(42) Serp, P.; Corrias, M.; Kalck, P. Carbon Nanotubes and Nanofibers in Catalysis. *Appl. Catal., A* **2003**, *253*, 337−358.

(43) Mondal, K. C.; Cele, L. M.; Witcomb, M. J.; Coville, N. J. Carbon Microsphere Supported Pd Catalysts for Hydrogenation of Ethylene. *Catal. Commun.* **2008**, *9*, 494−498.

(44) Pham-Huu, C.; Keller, N.; Charbonniere, L. J.; Ziesselb, R.; Ledoux, M. J. Carbon Nanofiber Supported Palladium Catalyst for Liquid-Phase Reactions. An Active and Selective Catalyst for Hydrogenation Of C=C Bonds. *Chem. Commun.* **2000**, 1871−1872.

(45) Rao, C. R. K.; Trivedi, D. C. Chemical and Electrochemical Depositions of Platinum Group Metals and Their Applications. *Coord. Chem. Rev.* **2005**, *249*, 613−631.

(46) Thiagarajan, S.; Yang, R.; Chen, S. Palladium Nanoparticles Modified Electrode for The Selective Detection of Catecholamine Neurotransmitters in Presence of Ascorbic Acid. *Bioelectrochemistry* **2009**, *75*, 163−169.

(47) Liu, S.; Li, H.; Shi, M.; Jiang, H.; Hu, X.; Li, W.; Fu, L.; Chen, H. Pd/C as a Clean and Effective Heterogeneous Catalyst for C−C Couplings toward Highly Pure Semiconducting Polymers. *Macro-molecules* **2012**, *45*, 9004−9009.

(48) Miyake, H.; Okada, T.; Samjeskéb, G.; Osawa, M. Formic Acid Electrooxidation on Pd in Acidic Solutions Studied by Surface-Enhanced Infrared Absorption Spectroscopy. *Phys. Chem. Chem. Phys.* **2008**, *10*, 3662−3669.

(49) Solis, V.; Iwasita, T.; Pavese, A.; Vielstich, W. Investigation of Formic Acid Oxidation on Palladium in Acidic Solutions by On-Line Mass Spectroscopy. *J. Electroanal. Chem. Interfacial Electrochem.* **1988**, *255*, 155.

(50) Pavese, A. G.; Solis, V. M.; Giordano, M. C. Oxidation of Formic Acid on Palladium Anodes in Acidic Medium. Effect of Pd (II) Ions. *Electrochim. Acta* **1987**, *32*, 1213−1216.

(51) Adić, R. R.; Spasojević, M. D.; Despić, A. R. Electrocatalysis by Foreign Metal Monolayers: Oxidation of Formic Acid on Palladium. *J. Electroanal. Chem. Interfacial Electrochem.* **1978**, *92*, 31−43.

(52) Zhu, Y.; Khan, Z.; Masel, R. I. The Behavior of Palladium Catalysts in Direct Formic Acid Fuel Cells. *J. Power Sources* **2005**, *139*, 15−20.

(53) Ha, S.; Larsen, R.; Masel, R. I. Performance characterization of Pd/C nanocatalyst for direct formic acid fuel cells. *J. Power Sources* **2005**, *144*, 28−34.

(54) Wang, T.; Chutia, A.; Brett, D. J. L.; Shearing, P. R.; He, G.; Chai, G.; Parkin, I. P. Palladium Alloys Used as Electrocatalysts for The Oxygen Reduction Reaction. *Energy Environ. Sci.* **2021**, *14*, 2639−2669.

(55) Erikson, H.; Sarapuu, A.; Tammeveski, K.; Solla-Gullón, J.; Feliu, J. M. Enhanced Electrocatalytic Activity of Cubic Pd Nanoparticles Towards the Oxygen Reduction Reaction in Acid Media. *Electrochem. Commun.* **2011**, *13*, 734−737.

(56) Erikson, H.; Sarapuu, A.; Alexeyeva, N.; Tammeveski, K.; Solla-Gullón, J.; Feliu, J. M. Electrochemical Reduction of Oxygen on Palladium Nanocubes in Acid and Alkaline Solutions. *Electrochim. Acta* **2012**, *59*, 329−335.

(57) Lüsi, M.; Erikson, H.; Sarapuu, A.; Tammeveski, K.; Solla-Gullón, J.; Feliu, J. M. Oxygen Reduction Reaction on Carbon-Supported Palladium Nanocubes in Alkaline Media. *Electrochem. Commun.* **2016**, *64*, 9−13.

(58) Wang, X.; Li, Z.; Qu, Y.; Yuan, T.; Wang, W.; Wu, Y.; Li, Y. Review of Metal Catalysts for Oxygen Reduction Reaction: From Nanoscale Engineering to Atomic Design. *Chem* **2019**, *5*, 1486−1511.

(59) Chen, A.; Ostrom, C. Palladium-Based Nanomaterials: Synthesis and Electrochemical Applications. *Chem. Rev.* **2015**, *115*, 11999−12044.

(60) Aarzoo; Nidhi; Samim, M. Palladium Nanoparticles as Emerging Pollutants from Motor Vehicles: An In-Depth Review on Distribution, Uptake and Toxicological Effects in Occupational and Living Environment. *Sci. Total Environ.* **2022**, *823*, No. 153787.

(61) Leśniewska, B. A.; Godlewska-Żyłkiewicz, B.; Bocca, B.; Caimi, S.; Caroli, S.; Hulanicki, A. Platinum, Palladium and Rhodium Content in Road Dust, Tunnel Dust and Common Grass in Biaystok Area (Poland): A Pilot Study. *Sci. Total Environ.* **2004**, *321*, 93−104.

(62) Gómez, B.; Palacios, M. A.; Gómez, M.; Sanchez, J. L.; Morrison, G.; Rauch, S.; McLeod, C.; Ma, R.; Caroli, S.; Alimonti, A.; Petrucci, F.; Bocca, B.; Schramel, P.; Zischka, M.; Petterson, C.; Wass, U. Levels and Risk Assessment for Humans and Ecosystems Of Platinum-Group Elements In The Airborne Particles And Road Dust Of Some European Cities. *Sci. Total Environ.* **2002**, *299*, 1−19.

(63) Helmers, E.; Schwarzer, M.; Schuster, M. Comparison of Palladium and Platinum in Environmental Matrices: Palladium Pollution by Automobile Emissions? *Environ. Sci. Pollut. Res.* **1998**, *5*, 44−50.

(64) Boch, K.; Schuster, M.; Risse, G.; Schwarzer, M. Microwave-Assisted Digestion Procedure for The Determination of Palladium in Road Dust. *Anal. Chim. Acta* **2002**, *459*, 257−265.

(65) Lottermoser, B. G. Noble Metals in Municipal Sewage Sludges of Southeastern Australia. *Ambio* **1995**, *24*, 354−357.

(66) Mansor, N.; Mohamed, N.; Suah, F. B. M. Electrochemical Recovery of Low Concentration of Palladium from Palladium (II) Chloride of Electroplating Wastewater. *J. Chem. Technol. Biotechnol.* **2021**, *96*, 3216−3223.

(67) Melber, C.; Keller, D.; Mangelsdorf, I. *Palladium*; World Health Organization: Geneva, 2002; pp. 3−5.

(68) Moore, J. W.; Hall, L.; Campbell, K.; Stara, J. Preliminary Studies on The Toxicity and Metabolism of Palladium and Platinum. Environ Health Perspect. *Environ. Health Perspect.* **1975**, *10*, 63−71.

(69) Hassanien, M. M.; Mortada, W. I.; Kenawy, I. M. Selective Separation of Palladium from Synthetic Highly Active Liquid Waste By Cloud Point Extraction Using Benzil Mono-(2-Pyridyl)

Hydrazone And Triton X-114. *J. Radioanal. Nucl. Chem.* **2014**, *303*, 261−269.

(70) Rosso, J. P. Maximize Precious Metal Recovery from Spent Catalysts. *Chem. Eng. Prog.* **1992**, *88*, 66.

(71) Lassner, J. A.; Lasher, L. B.; Koppel, R. L.; Hamilton, J. N. Reclaim Spent Catalysts Properly. *Chem. Eng. Prog.* **1994**, *90*, 95.

(72) Le, M. N.; Lee, M. S. A Review on Hydrometallurgical Processes for The Recovery of Valuable Metals From Spent Catalysts And Life Cycle Analysis Perspective. *Miner. Process. Extr. Metall. Rev.* **2020**, *42*, 335−354.

(73) Sethurajan, M.; Hullebusch, E. D. V.; Fontana, D.; Akcil, A.; Deveci, H.; Batinic, B.; Leal, J. P.; Gasche, T. A.; Kucuker, M. A.; Kuchta, K.; Neto, I. F. F.; Soares, H. M. V. M.; Chmielarz, A. Recent Advances on Hydrometallurgical Recovery of Critical and Precious Elements from End of Life Electronic Wastes - A Review. *Crit. Rev. Environ. Sci. Technol.* **2019**, *49*, 212−275.

(74) Hoffmann, J. E. Recovery of Platinum-Group Metals from Gabbroic Rocks Metals from Auto Catalysts. *JOM* **1988**, *40*, 40−44.

(75) Bourgeois, D.; Lacanau, V.; Mastretta, R.; Contino-Pépin, C.; Meyer, D. A Simple Process for The Recovery of Palladium from Wastes of Printed Circuit Boards. *Hydrometallurgy* **2020**, *191*, No. 105241.

(76) Zhang, Z.; Zhang, S. Selective Recovery of Palladium from Waste Printed Circuit Boards by A Novel Non-Acid Process. *J. Hazard. Mater.* **2014**, *279*, 46−51.

(77) Yazici, E. Y.; Deveci, H. Extraction of Metals from Waste Printed Circuit Boards (WPCBs) in H_2SO_4−$CuSO_4$−NaCl Solutions. *Hydrometallurgy* **2013**, *139*, 30−38.

(78) Prabaharan, G.; Barik, S. P.; Kumar, B. A Hydrometallurgical Process for Recovering Total Metal Values from Waste Monolithic Ceramic Capacitors. *Waste Manage.* **2016**, *52*, 302−308.

(79) Fontana, D.; Pietrantonio, M.; Pucciarmati, S.; Torelli, G. N.; Bonomi, C.; Masi, F. Palladium Recovery from Monolithic Ceramic Capacitors by Leaching, Solvent Extraction and Reduction. *J. Mater. Cycles Waste Manag.* **2018**, *20*, 1199−1206.

(80) Behnamfard, A.; Salarirad, M.; Veglio, F. Process Development for Recovery of Copper and Precious Metals from Waste Printed Circuit Boards with Emphasize on Palladium and Gold Leaching and Precipitation. *Waste Manage.* **2013**, *33*, 2354−2363.

(81) Ponou, J.; Wang, L. P.; Dodbiba, G.; Fujita, T. Separation of Palladium and Silver from Semiconductor Solid Waste by Means of Liquid-Liquid-Powder Extraction Using Dodecyl Amine Acetate as A Surfactant Collector. *Sep. Purif. Technol.* **2018**, *191*, 86−93.

(82) Liu, K.; Zhang, Z.; Zhang, F. Direct Extraction of Palladium and Silver from Waste Printed Circuit Boards Powder by Supercritical Fluids Oxidation-Extraction Process. *Hazard. Mater.* **2016**, *318*, 216−223.

(83) Xiu, F.; Qi, Y.; Zhang, F. Leaching of Au, Ag, And Pd from Waste Printed Circuit Boards of Mobile Phone by Iodide Lixiviant After Supercritical Water Pre-Treatment. *Waste Manage.* **2015**, *41*, 134−141.

(84) Singh, L.; Mahapatra, D. A.; Thakur, S. Bioelectrochemical systems for removal and recovery of heavy metals. In *Bioremediation, nutrients, and other valuable product recovery*; Elsevier, 2020; pp. 185−203.

(85) Fu, F.; Wang, Q. Removal of Heavy Metal Ions from Wastewaters: A Review. *J. Environ. Manage.* **2011**, *92*, 407−418.

(86) Thakkar, K. N.; Mhatre, S. S.; Parikh, R. Y. Biological Synthesis of Metallic Nanoparticles. *Nanomedicine* **2010**, *6*, 257−262.

(87) Virkutyte, J.; Varma, R. S. Green Synthesis of Metal Nanoparticles: Biodegradable polymers and enzymes in stabilization and surface functionalization. *Chem. Sci.* **2011**, *2*, 837−846.

(88) Alemu, T.; Assresahegn, B. D.; Soreta, T. R. Tuning the Initial Electronucleation Mechanism of Palladium on Glassy Carbon Electrode. *Port. Electrochim. Acta.* **2014**, *32*, 21−33.

(89) Meunier, N.; Drogui, P.; Montané, C.; Hausler, R.; Mercier, G.; Blais, J. Comparison Between Electrocoagulation and Chemical Precipitation for Metals Removal from Acidic Soil Leachate. *J. Hazard. Mater.* **2006**, *137*, 581−590.

(90) Zhang, C.; Jiang, Y.; Li, Y.; Hu, Z.; Zhou, L.; Zhou, M. three-dimensional electrochemical process for wastewater treatment: A General Review. *Chem. Eng. J.* **2013**, *228*, 455−467.

(91) Tran, T. K.; Leu, H. J.; Chiu, K. F.; Lin, C. Y. Electrochemical Treatment of Heavy Metal-Containing Wastewater with The Removal of COD and Heavy Metal Ions. *Chem. Soc.* **2017**, *64*, 493−502.

(92) Saji, V. S.; Cook, R. Electrodeposition: the versatile technique for nanomaterials. In *Corrosion protection and control using nanomaterials*; Woodhead Publishing, 2016; pp. 86−125.

(93) Benea, L. Surface Modifications of Materials by Electrochemical Methods to Improve the Properties for Industrial and Medical Applications. *IOP Conf. Ser.: Mater. Sci. Eng.* **2018**, *374*, No. 012014.

(94) Nasirpouri, F.; Alipour, K.; Daneshvar, F.; Sanaeian, M.-R. Electrodeposition of anticorrosion nanocoatings. In *Corrosion Protection at the Nanoscale*; Elsevier, 2020; pp. 473−497.

(95) Jing, M.; Wu, T.; Zou, G.; Hou, H.; Ji, X. Nanomaterials for Electrochemical Energy Storage. *Front. Nanosci.* **2021**, *18*, 421−484.

(96) Chang, J. H.; Ellis, A. V.; Yan, C. T.; Tung, C. H. The Electrochemical Phenomena and Kinetics of EDTA−Copper Wastewater Reclamation by Electrodeposition and Ultrasound. *Sep. Purif. Technol.* **2009**, *68*, 216−221.

(97) Colantonio, N.; Kim, Y. Cadmium (II) Removal Mechanisms in Microbial Electrolysis Cells. *J. Hazard. Mater.* **2016**, *311*, 134−141.

(98) Farooq, R.; Wang, Y.; Lin, F.; Shaukat, S. F.; Donaldson, J.; Chouhdary, A. J. Effect of Ultrasound on The Removal of Copper from the Model Solutions for Copper Electrolysis Process. *Water Res.* **2002**, *36*, 3165−3169.

(99) Shao, M.; Li, S.; Jin, C.; Chen, M.; Huang, Z. Recovery of Pd (II) From Hydrochloric Acid Medium by Solvent Extraction−Direct Electrodeposition Using Hydrophilic/Hydrophobic Ils. *ACS Omega* **2020**, *5*, 27188−27196.

(100) Terrazas-Rodríguez, J. E.; Gutiérrez-Granados, S.; Alatorre-Ordaz, M. A.; Ponce de León, C.; Walsh, F. C. A Comparison of The Electrochemical Recovery of Palladium Using a Parallel Flat Plate Flow-By Reactor and A Rotating Cylinder Electrode Reactor. *Electrochim. Acta* **2011**, *56*, 9357−9363.

(101) Marshall, R. J.; Walsh, F. C. Review of Some Recent Electrolytic Cell Designs. *Surf. Technol.* **1985**, *24*, 45−77.

(102) Robbs, P. H.; Rees, N. V. Nanoparticle Electrochemistry. *Phys. Chem. Chem. Phys.* **2016**, *18*, 24812−24819.

(103) Allerston, L. K.; Rees, N. V. Nanoparticle Impacts in Innovative Electrochemistry. *Curr. Opin. Electrochem.* **2018**, *10*, 31−36.

(104) Kahk, J. M.; Rees, N. V.; Pillay, J.; Tshikhudo, R.; Vilakazi, S.; Compton, R. Electron Transfer Kinetics at Single Nanoparticles. *Nano Today* **2012**, *7*, 174−179.

(105) Korshunov, A.; Heyrovský, M. Voltammetry of Metallic Powder Suspensions on Mercury Electrodes. *Electroanalysis* **2006**, *18*, 423−426.

(106) Saw, E. N.; Blanc, N.; Kanokkanchana, K.; Tschulik, K. Time-Resolved Impact Electrochemistry - A New Method to Determine Diffusion Coefficients of Ions in Solution. *Electrochim. Acta* **2018**, *282*, 317−323.

(107) Pumera, M. Impact Electrochemistry: Measuring Individual Nanoparticles. *ACS Nano* **2014**, *8*, 7555−7558.

(108) Zhou, Y. G.; Rees, N. V.; Compton, R. G. The Electrochemical Detection and Characterization of Silver Nanoparticles in Aqueous Solution. *Angew. Chem. Int. Ed.* **2011**, *50*, 4219−4221.

(109) Rees, N. V.; Zhou, Y. G.; Compton, R. G. The Aggregation of Silver Nanoparticles in Aqueous Solution Investigated Via Anodic Particle Coulometry. *ChemPhysChem* **2011**, *12*, 1645−1647.

(110) Haddou, B.; Rees, N. V.; Compton, R. G. Nanoparticle−Electrode Impacts: The Oxidation of Copper Nanoparticles Has Slow Kinetics. *Phys. Chem. Chem. Phys.* **2012**, *14*, 13612.

(111) Zhou, Y. G.; Haddou, B.; Rees, N. V.; Compton, R. G. The Charge Transfer Kinetics of The Oxidation of Silver and Nickel Nanoparticles Via Particle−Electrode Impact Electrochemistry. *Phys. Chem. Chem. Phys.* **2012**, *14*, 14354.

(112) Tschulik, K.; Haddou, B.; Omanović, D.; Rees, N.; Compton, R. Coulometric Sizing of Nanoparticles: Cathodic and Anodic Impact Experiments Open Two Independent Routes to Electrochemical Sizing of Fe_3O_4 Nanoparticles. *Nano Res.* 2013, 6, 836–841.

(113) Nasir, M.; Pumera, M. Impact Electrochemistry on Screen-Printed Electrodes for The Detection of Monodispersed Silver Nanoparticles of Sizes 10–107 Nm. *Phys. Chem. Chem. Phys.* 2016, 18, 28183–28188.

(114) Teo, W. Z.; Pumera, M. Fate of silver nanoparticles in natural waters; integrative use of conventional and electrochemical analytical techniques. *RSC Adv.* 2014, 4, 5006–5011.

(115) Stuart, E. J. E.; Zhou, Y. G.; Rees, N. V.; Compton, R. Determining Unknown Concentrations of Nanoparticles: The Particle-Impact Electrochemistry of Nickel and Silver. *RSC Adv.* 2012, 2, 6879–6884.

(116) Lim, C. S.; Pumera, M. Impact Electrochemistry: Colloidal Metal Sulfide Detection by Cathodic Particle Coulometry. *Phys. Chem. Chem. Phys.* 2015, 17, 26997–27000.

(117) Kwon, S. J.; Bard, A. J. Analysis of Diffusion-Controlled Stochastic Events of Iridium Oxide Single Nanoparticle Collisions by Scanning Electrochemical Microscopy. *J. Am. Chem. Soc.* 2012, 134, 7102–7108.

(118) Xiao, X.; Fan, F. R.; Zhou, J.; Bard, A. J. Current Transients in Single Nanoparticle Collision Events. *J. Am. Chem. Soc.* 2008, 130, 16669–16677.

(119) Stuart, E. J. E.; Rees, N. V.; Compton, R. G. Particle-Impact Voltammetry: The Reduction of Hydrogen Peroxide at Silver Nanoparticles Impacting a Carbon Electrode. *Chem. Phys. Lett.* 2012, 531, 94–97.

(120) Zhou, Y. G.; Rees, N. V.; Compton, R. G. The Electro-chemical Detection of Tagged Nanoparticles Via Particle-Electrode Collisions: Nanoelectroanalysis Beyond Immobilisation. *Chem. Commun.* 2012, 48, 2510–2512.

(121) Kwon, S. J.; Fan, F. R. F.; Bard, A. J. Observing Iridium Oxide (Irox) Single Nanoparticle Collisions at Ultramicroelectrodes. *J. Am. Chem. Soc.* 2010, 132, 13165–13167.

(122) Kwon, S. J.; Zhou, H.; Fan, F.-R. F.; Vorobyev, V.; Zhang, B.; Bard, A. J. Stochastic Electrochemistry with Electrocatalytic Nanoparticles at Inert Ultramicroelectrodes—Theory and Experiments. *Phys. Chem. Chem. Phys.* 2011, 13, 5394–5402.

(123) Zhou, Y. G.; Rees, N. V.; Compton, R. G. Electrochemistry of Nickel Nanoparticles Is Controlled by Surface Oxide Layers. *Phys. Chem. Chem. Phys.* 2013, 15, 761–763.

(124) Rees, N. V. Electrochemical Insight from Nanoparticle Collisions with Electrodes: A Mini-Review. *Electrochem. Commun.* 2014, 43, 83–86.

(125) Stuart, E. J. E.; Zhou, Y. G.; Rees, N. V.; Compton, R. G. Particle-impact nanoelectrochemistry: A Fickian model for nanoparticle transport. *RSC Adv.* 2012, 2, 12702–12705.

(126) Cheng, W.; Zhou, X. F.; Compton, R. G. Electrochemical Sizing of Organic Nanoparticles. *Angew. Chem., Int. Ed.* 2013, 125, 13218–13220.

(127) Cheng, W.; Batchelor-McAuley, C.; Compton, R. G. Organic Nanoparticles: Mechanism of Electron Transfer to Indigo Nano-particles. *ChemElectroChem* 2014, 1, 714–717.

(128) Xiao, X.; Bard, A. J. Observing Single Nanoparticle Collisions at An Ultramicroelectrode by Electrocatalytic Amplification. *J. Am. Chem. Soc.* 2007, 129, 9610–9612.

(129) Giovanni, M.; Ambrosi, A.; Sofer, Z.; Pumera, M. Impact Electrochemistry of Individual Molybdenum Nanoparticles. *Electrochem. Commun.* 2015, 56, 16–19.

(130) Zampardi, G.; Compton, R. G. Fast Electrodeposition of Zinc onto Single Zinc Nanoparticles. *J. Solid State Electrochem.* 2020, 24, 2695–2702.

(131) Zhou, Y. G.; Rees, N. V.; Compton, R. G. Nanoparticle-Electrode Collision Processes: The Underpotential Deposition of Thallium on Silver Nanoparticles in Aqueous Solution. *ChemPhysChem* 2011, 12, 2085–2087.

(132) Zhou, Y. G.; Rees, N. V.; Compton, R. G. Nanoparticle–Electrode Collision Processes: The Electroplating of Bulk Cadmium on Impacting Silver Nanoparticles. *Chem. Phys. Lett.* 2011, 511, 183–186.

(133) Oladeji, A. V.; Courtney, J. M.; Rees, N. V. Copper Deposition on Metallic and Non-Metallic Single Particles Via Impact Electrochemistry. *Electrochim. Acta* 2022, 405, No. 139838.

(134) Kanokkanchana, K.; Saw, E. N.; Tschulik, K. Nano Impact Electrochemistry: Effects of Electronic Filtering on Peak Height, Duration and Area. *ChemElectroChem* 2018, 5, 3000–3005.

(135) Jiao, X.; Batchelor-McAuley, C.; Lin, C.; Kätelhön, E.; Tanner, E.; Young, N. P.; Compton, R. G. Role of Nanomorphology and Interfacial Structure of Platinum Nanoparticles in Catalyzing the Hydrogen Oxidation Reaction. *ACS Catal.* 2018, 8, 6192–6202.

(136) Tschulik, K.; Batchelor-McAuley, C.; Toh, H. S.; Stuart, E.; Compton, R. G. Electrochemical Studies of Silver Nanoparticles: A Guide for Experimentalists and A Perspective. *Phys. Chem. Chem. Phys.* 2014, 16, 616–623.

(137) Voiry, D.; Chhowalla, M.; Gogotsi, Y.; Kotov, N. A.; Li, Y.; Penner, R. M.; Schaak, R. E.; Weiss, P. S. Best Practices for Reporting Electrocatalytic Performance of Nanomaterials. *ACS Nano* 2018, 12, 9635–9638.

(138) Sanchis-Gual, R.; Seijas-Da Silva, A. S. D.; Coronado-Puchau, M.; Otero, T. F.; Abellán, G.; Coronado, E. Improving the Onset Potential and Tafel Slope Determination of Earth-Abundant Water Oxidation Electrocatalysts. *Electrochim. Acta* 2021, 388, No. 138613.

(139) Andersen, J. E. T.; Bech-Nielsen, G.; Møller, P.; Reeve, J. C. Bulk Copper Electrodeposition on Gold Imaged by In Situ STM: Morphology and Influence of Tip Potential. *J. Appl. Electrochem.* 1996, 26, 161–170.

(140) Bell, M. F.; Harrison, J. A. The deposition of palladium. *J. Electroanal. Chem. Interfacial Electrochem.* 1973, 41, 15–25.

(141) Maniam, K. K.; Muthukumar, V.; Chetty, R. Electrodeposition of Dendritic Palladium Nanostructures on Carbon Support for Direct Formic Acid Fuel Cells. *J. Hydrogen Energy.* 2016, 41, 18602–18609.

(142) Heydari, H.; Abdolmaleki, A.; Gholivand, M. B. Electro-deposition and characterization of palladium nanostructures on stainless steel and application as hydrogen sensor. *Ciência E Natura* 2015, 37, 23–33.

(143) Smirnov, M. Y.; Klembovskii, I. O.; Kalinkin, A. V.; Bukhtiyarov, V. I. An XPS Study of the Interaction of a Palladium Foil with NO_2. *Kinet. Catal.* 2018, 59, 786–791.

(144) Militello, M. C.; Simko, S. J. Elemental Palladium By XPS. *Surf. Sci. Spectra* 1994, 3, 387–394.

(145) Briggs, D.; Seah, M. P. *Practical Surface Analysis, Auger and X-ray Photoelectron Spectroscopy*; 2nd edition; John Wiley & Sons, 1990; Vol. 1, pp. 595–641.

(146) Moulder, J. F.; Stickle, W. F.; Sobol, P. E.; Bomben, K. D. *Handbook of X-ray Photoelectron Spectroscopy*; Chastain, J., Ed.; Perkin-Elmer, 1992: pp. 118–119

(147) Kim, K. S.; Gossmann, A. F.; Winograd, N. X-ray photoelectron spectroscopic studies of palladium oxides and the palladium-oxygen electrode. *Anal. Chem.* 1974, 46, 197–200.

(148) Militello, M. C.; Simko, S. J. Palladium Oxide (PdO) By XPS. *Surf. Sci. Spectra* 1994, 3, 395–401.

(149) Militello, M. C.; Simko, S. J. Palladium Chloride ($PdCl_2$) By XPS. *Surf. Sci. Spectra* 1994, 3, 402–409.

(150) Meng, H.; Wang, C.; Shen, P. K.; Wub, G. Palladium thorn clusters as catalysts for electrooxidation of formic acid. *Energy Environ. Sci.* 2011, 4, 1522–1526.

(151) Wheeler, D. L.; Barrett, T.; Benson, D. A.; Bryant, S. H.; Canese, K.; Chetvernin, V.; Church, D. M.; DiCuccio, M.; Edgar, R.; Federhen, S.; Geer, L. Y.; Kapustin, Y.; Khovayko, O.; Landsman, D.; Lipman, D. J.; Madden, T. L.; Maglott, D. R.; Ostell, J.; Miller, V.; Pruitt, K. D.; Schuler, G. D.; Sequeira, E.; Sherry, S. T.; Sirotkin, K.; Souvorov, A.; Starchenko, G.; Tatusov, R. L.; Tatusova, T. A.; Wagner, L.; Yaschenko, E. Database resources of the National Center for Biotechnology Information. *Nucleic Acids Res.* 2007, 35, D5–D12.

(152) Ulrich, E. L.; Akutsu, H.; Doreleijers, J. F.; Harano, Y.; Ioannidis, Y. E.; Lin, J.; Livny, M.; Mading, S.; Maziuk, D.; Miller, Z.; Nakatani, E.; Schulte, C. F.; Tolmie, D. E.; Wenger, R. K.; Yao, H.; Markley, J. L. BioMagResBank. *Nucleic Acids Res.* **2008**, *36*, D402–D408.

(153) Wilschefski, S. C.; Baxter, M. R. Inductively Coupled Plasma Mass Spectrometry: Introduction to Analytical Aspects. *Clin. Biochem. Rev.* **2019**, *40*, 115–133.

(154) Olivares, J. A.; Houk, R. S. Suppression of Analyte Signal by Various Concomitant Salts in Inductively Coupled Plasma Mass Spectrometry. *Anal. Chem.* **1986**, *58*, 20–25.